Astrocyte-mediated transduction of muscle fiber contractions synchronizes hippocampal neuronal network development

Ki Yun Lee[1], Justin S. Rhodes[2, *], and M. Taher A. Saif[1, *]

[1] Department of Mechanical Science and Engineering, University of Illinois at Urbana-Champaign, Urbana, IL 61801, USA

[2] Department of Psychology, Beckman Institute, University of Illinois at Urbana-Champaign, Urbana, IL 61801, USA

[*] Corresponding authors

Email: jrhodes@illinois.edu (JR), saif@illinois.edu (MS)

Abstract

Exercise supports brain health in part through enhancing hippocampal function. The leading hypothesis is that muscles release factors when they contract (e.g., lactate, myokines, growth factors) that enter circulation and reach the brain where they enhance plasticity (e.g., increase neurogenesis and synaptogenesis). However, it remains unknown how the muscle signals are transduced by the hippocampal cells to modulate network activity and synaptic development. Thus, we established an *in vitro* model in which the media from contracting primary muscle cells (CM) is applied to developing primary hippocampal cell cultures on a microelectrode array. We found that the hippocampal neuronal network matures more rapidly (as indicated by synapse development and synchronous neuronal activity) when exposed to CM than regular media (RM). This was accompanied by a fourfold increase in the proliferation of astrocytes. Further, experiments established that the astrocytes release factors that inhibit neuronal excitability and facilitate network development. Results provide new insight into how exercise may support hippocampal function through regulating astrocyte proliferation and subsequent taming of neuronal activity into an integrated network.

Introduction

Exercise is a highly effective strategy for maintaining cognitive health throughout life, even when initiated at late stages in life [1–3]. Many studies have shown robust long-term changes in the hippocampus from increased physical activity, such as increased adult hippocampal neurogenesis, synaptogenesis and enlarged hippocampal volume which likely support enhanced cognition [3–7]. However, the mechanisms by which exercise produces such dramatic changes in the hippocampus remain elusive. Uncovering the mechanisms that are responsible for enlarging the hippocampus and enhancing its function could be used to reverse-engineer treatments for cognitive pathologies that result in a diminished size and function of the hippocampus, such as Alzheimer's disease, stress, depression, anxiety, PTSD, Cushing's disease, epilepsy, and normal aging [8].

Cumulative research over the past few decades has suggested that factors released from contracting muscles (such as lactate [9], growth factors [10,11], trophic factors [12], and myokines [13,14]) provide crucial signals that support enhanced plasticity [15]. However, how muscle factors affect hippocampal cells is still being worked out. Recently, we found that repeated electrical contractions of the hindlimb muscles of anesthetized mice in a pattern that produced endurance adaptations in the muscles (40 reps, twice a week for 8 weeks) caused increased numbers of new astrocytes in the hippocampus and enlarged the volume of the dentate gyrus by approximately 10% [16]. This suggests astrocytes are sensitive to muscle factors and proliferate when they detect muscle factors in the blood. Given the role that astrocytes play in forming the blood-brain barrier, they are well situated to transduce signals from the blood into the brain.

One way to study the interactions between contracting muscle cells and hippocampal cells including neurons and astrocytes is to isolate the cells and perform experiments *in vitro*. For example, previous *in vitro* studies found that muscle conditioned media attracted neurites of spinal cord motor neurons to form neuro-muscular junctions [17]. Along this line, our lab has been examining cross-talk between muscles and neurons *in vitro.* We recently found that when media from contracting muscle fibers derived from a C2C12 mouse myoblast cell line is applied to neuronal cultures derived from a mouse embryonic stem cell line plated on a micro-electrode array, it enhanced overall neural firing rates of the neurons [18].

To further explore how factors from contracting muscles might influence hippocampal cells, we developed an *in vitro* preparation in which primary mouse skeletal muscle cells are plated on a functionalized substrate. The myoblasts develop bundles of myotubes and begin to contract spontaneously. We then take the media surrounding the contracting muscles (conditioned media, CM) and apply that media to *in vitro* primary hippocampal cell cultures that include neurons and astrocytes. The objectives of this study were to determine whether CM influences the function and maturation of hippocampal neuronal networks, and to investigate the

64 role of astrocytes in the process of transduction of muscle contractions to the activity of hippocampal neuronal
65 networks *in vitro*.

Materials and methods

Primary mouse skeletal muscle and hippocampus dissection

Muscle tissues from the hindlimbs of 4-week-old CD1 mice were collected and dissociated using a standard protocol [19] with slight modifications. Briefly, the tissues were collected in cold DPBS (Corning), minced, and digested for 30 minutes in digestion media consisting of DMEM, 2.5% HEPES, 1% GlutaMAX (all from Gibco), and 1% Penicillin-Streptomycin (Lonza) with the addition of 400 unit/ml collagenase (Worthington) and 2.4 unit/ml dispase (Sigma). The remaining tissues were triturated by pipetting in 0.25% trypsin (Gibco), then filtered by 70 and 40 μm cell strainers. After the dissociation, the pre-plating technique [20,21] was implemented to remove fibroblasts and increase the yield of myoblasts. The pre-plating technique steps are following. First, the dissociated cells were plated and incubated in uncoated flasks for three hours. Second, the supernatant with floating cells was collected and transferred into functionalized culture dishes.

For hippocampal dissection, hippocampal tissues were isolated from 2-day-old CD1 mouse pups and dissociated into single cells by following established protocol [22]. The dissected hippocampal tissues were collected in cold Hibernate-E (Gibco), minced, then digested twice in 2 mg/ml papain (Sigma) for 30 minutes. The remaining tissues were mechanically dissociated further by pipetting, then filtered by 70 and 40 μm cell strainers.

All procedures were approved by the University of Illinois Institutional Animal Care and Use Committee and adhered to NIH guidelines (protocol number: 21053).

Cell culture

Culture dishes were coated with 0.1 mg/ml Matrigel (Corning) for preparations of cell culture. The primary skeletal myoblasts were maintained below 70~80% confluency in muscle growth media consisting of Ham's F-10 Nutrient Mix, 20% fetal bovine serum, 1% GlutaMAX, 1% MEM Non-Essential Amino Acids (all from Gibco), 1% Penicillin-Streptomycin, and 0.5% chick embryo extract (US Biological) with ice-cold 10 ng/ml bFGF, 20 μM forskolin, and 100 μM IBMX (all reagent from Sigma). Once the confluency reached 70~80%, then the culture was maintained in muscle differentiation media consisting of DMEM and Ham's F-12 Nutrient Mix at a volume ratio of 1:1, 10% horse serum, 1% GlutaMAX (all from Gibco), and 1% Penicillin-Streptomycin to initiate myotube formations. Once myotubes were matured and contractions were observed, the media was changed with pre-muscle conditioned media consisting of Advanced DMEM/F-12, 1% GlutaMAX (all from Gibco), and 1% Penicillin-Streptomycin.

For the hippocampal neuron culture, the preparation of cell culture is the same as muscle culture. Hippocampal neuron cells were cultured using specially formulated media by the lab such as RM, CM, astrocyte media

conditioned by RM (Ast-RM), and astrocyte media conditioned by CM (Ast-CM) depending on experiments (see details in Materials and methods).

Muscle anti-actomyosin and glia anti-mitotic treatments

To inhibit skeletal muscle contraction, the specific reagent was used as shown in previous studies [23,24]. In the fully differentiated muscle culture with spontaneous contraction, 10 μM *N*-benzyl-*p*-toluene sulphonamide (BTS) (Sigma) was added. After 5-6 days, the BTS solution was replenished with the control media with 0 μM BTS and tension recovery was monitored after the washout.

In the mechanistic study, the proliferation of glia was inhibited by the specific reagent using the standard protocol [25]. Briefly, culture was treated with a cocktail consisting of 20 μM 5-fluorodeoxyuridine (MP Biomedicals), 20 μM uridine, and 0.5 μM Arabinofuranosyl Cytidine (all from Sigma) on day 1 and incubated for 72 hours. After 72 hours, 2/3 of the media was replenished with new media without the cocktail. A day after, the whole media was changed without the cocktail.

Collection of muscle and astrocyte conditioned media

For the collection of RM and CM, primary skeletal myoblasts were cultured in muscle growth media, then muscle differentiation media when the confluency reaches 70~80%. Once myotubes were matured and 10~20% of myotubes began to twitch autonomously which is about 4 days after, the culture was maintained in pre-muscle conditioned media. The pre-muscle conditioned media was collected using 0.22 μm filters every 24 hours for 8 days and stored at -80 °C. For control, pre-regular media was collected from a culture dish without muscle cells, treated, incubated, and stored the same way as the CM. The final forms of RM and CM consist of pre-regular and muscle conditioned media, respectively and Neurobasal medium at a volume ratio of 1:1, 10% KnockOut serum replacement, 1% GlutaMAX (all from Gibco), and 1% Penicillin-Streptomycin with ice-cold 0.1 mM β-mercaptoethanol (Gibco), 10 ng/ml glial-derived neurotrophic factor (Neuromics), and 10 ng/ml ciliary neurotrophic factor (Sigma).

For the collection of Ast-RM and Ast-CM, primary hippocampal neurons and astrocytes were cultured in basal media consisting of Advanced DMEM/F-12 and Neurobasal medium at a volume ratio of 1:1 10% KnockOut serum replacement, 1% GlutaMAX, and 1% Penicillin-Streptomycin. Once the confluency reached 100%, the media was replenished with RM and CM for the collection of Ast-RM and Ast-CM, respectively. The media was collected using 0.22 μm filters every 24 hours and stored at -80 °C.

Immunofluorescence

Immunocytochemistry was performed by following steps. Samples were fixed with 4% paraformaldehyde, permeabilized with 0.05% Triton-X for 15 minutes at room temperature, and blocked with buffer solution

consisting of DPBS, 5% goat serum (Sigma), and 1% bovine serum albumin (Sigma) overnight at 4 °C. The samples were treated with primary antibodies overnight at 4 °C, secondary antibodies for 2 hours, and DAPI (1:1000; Invitrogen, D1306) for 20 minutes at room temperature.

Primary antibodies were anti-synaptophysin monoclonal rabbit (1:1000; Abcam, ab32127), anti-PSD95 monoclonal mouse (1:1000; Invitrogen, MA1-046), anti-Bassoon monoclonal mouse (1:1000; Abcam, ab82958), anti-β III Tubulin polyclonal rabbit (1:1000; SYSY, 302 302), anti-S100β monoclonal mouse (1:1000; SYSY, 287 011), and Alexa Fluor 647-conjugated Phalloidin (1:500; Invitrogen, A22287). Secondary antibodies were goat anti-chicken IgY Alexa Fluor 488 (ab150173), goat anti-mouse IgY Alexa Fluor 488 (ab150117), goat anti-rabbit IgY Alexa Fluor 568 (ab175696), and goat anti-mouse IgY Alexa Fluor 647 (ab150119) (all 1:500; Abcam).

All samples were imaged using Zeiss 710 Confocal microscope (Carl Zeiss Microscopy).

Synapse detection using double-fluorescent label method

To detect and measure synapses and filamentous actin at presynaptic terminals, the double-fluorescent label method was used by following protocol with modifications [26]. Briefly, synapses or F-actin were double-labeled with two different antibodies at different channels. One set of puncta from one channel and the other set from the other channel were colocalized, then verified as synapses. The total intensity of synapse and F-actin was measured from integrated image planes after the colocalization process. The analysis was performed by ImageJ.

Calcium Imaging

Calcium imaging was performed using Cal-590-AM (AAT Bioquest, 20510) by the manufacturer's protocols. Briefly, samples were incubated with DMEM, 0.04% Pluronic F-127 (Sigma), and 5 µM Cal-590-AM for an hour at 37°C. After washout, samples were supplemented with DMEM with no phenol red to reduce background noise. The dye-loaded cells were excited at 574 nm and imaging was performed at the frame rate of 12 fps. For quantitative analysis, the average fluorescence intensity of selected regions of interest was calculated. Then the trace of fluorescent dynamics was calculated as $\Delta F/F_0 = (F_n - F_0)/F_0$, where where F_n and F_0 is the average intensity at n^{th} frame and at resting state, respectively.

MEA preparation

MEA measurements were performed using an MEA 2,100-Lite Amplifier (Multi Channel Systems MCS GmbH). The 6-well MEA device was fabricated from a manufacturer (Multi Channel Systems MCS GmbH), and it contained nine embedded 30 µm diameter TiN electrodes per well with 200 µm spacing between electrodes and six reference electrodes. The MEA device was coated with 0.1 mg/ml Poly-D-Lysine (Sigma)

and Matrigel for cell culture preparation. The cell seeding density for cultures in MEAs was 0.4-0.6 M/cm^2. Measurements were performed at a sampling rate of 10 kHz for 5 min at 37 °C with a sealed cover to keep CO_2 concentration stable. Media was replenished every other day.

MEA recording, and spike/burst detection

Neuronal activity was analyzed by Multi-Channel Analyzer software (Multi Channel Systems MCS GmbH), Python (3.9.7), and MATLAB. Raw data were filtered using a 2nd order Butterworth high pass filter with 200 Hz cutoff frequency. Action potentials were detected as spikes by a threshold of 4 × standard deviations for both rising and falling edge from the noise magnitude distribution. Spikes were only detected by active electrodes which were defined by electrodes containing at least 5 spikes/min. The parameters of burst detection are as follows: Maximum interval to start burst: 50 ms, maximum interval to end burst: 50 ms, minimum interval between bursts: 100 ms, minimum duration of burst: 50 ms, minimum number of spikes in burst: 4.

Synchrony index

The synchrony of spike trains between electrodes was assessed through cross-correlation for discrete functions [27]. There are total nine electrodes and spike train data for each electrode was cross-correlated with every other electrode. The synchrony index was achieved by averaging of 36 possible combinations. The cross-correlation was proceeded with zero lag. The synchrony index, $\bar{\chi}$, of nine electrodes is described as

$$\bar{\chi} = \frac{1}{36}\sum_{p=1}^{9}\sum_{q=p+1}^{9}\frac{\sum\left(x_i^p \cdot y_i^q\right)}{\sqrt{\sum\left(x_i^p\right)^2 \cdot \sum\left(y_i^q\right)^2}}$$

where x and y are spike trains consisting of 0 (no spike) and 1 (spike), p and q are the p^{th} and q^{th} electrode, and i is the i^{th} discrete time. $\bar{\chi} = 0$ and $\bar{\chi} = 1$ represent completely asynchronous and synchronous, respectively.

Statistical analysis

SAS (9.4) and R (4.0.3) were used for statistical analysis. $p < 0.05$ was considered statistically significant. Data were considered normally distributed when the absolute value of the skewness and kurtosis was less than 1 and 2, respectively. In the case of non-normal distribution, a power transform was used to transform data to meet the normality conditions. Actin intensity, muscle contraction amplitudes, calcium signal, and astrocyte number in response to the glia inhibitor were evaluated by two-sample t-test (RM vs. CM, control vs. BTS 10 μM, and control vs. glia inhibitor). Synapse number, vesicle accumulation, and astrocyte number were evaluated by two-way ANOVA with day (day 2 vs. day 9) and treatment (CM vs. RM) as factors. The MEA outcomes of the BTS study were analyzed using repeated measures three-way ANOVA with cohort as a blocking variable, day (day 2 to 9) entered as a within-subjects, muscle treatment (2 levels: RM vs. CM) as a between-subjects factor, and drug (2 levels: control vs. BTS) entered as a between-subjects factor. Similarly, the MEA outcomes of the glia reduced study were analyzed using repeated measures three-way ANOVA with cohort as a blocking variable,

190 day (day 2 to 9) entered as a within-subjects, muscle treatment (2 levels: RM vs. CM) as a between-subjects
191 factor, and astrocyte composition (3 levels: presence vs. absence vs. absence with astrocyte releasate (Ast-RM
192 and Ast-CM)) as a between-subjects factor. For the burst rate (BTS and glia reduced study) and synchrony
193 index (glia reduced study), aligned rank transform was used for the non-parametric test since data were
194 considered non-normally distributed. Post-hoc pairwise differences between means were performed using
195 Fisher's least significant difference test.

Results

Contracting muscle conditioned media enhances neuronal activity measured by microelectrode arrays

Consistent with our previous MEA study with C2C12 mouse myoblast cell line and mouse embryonic stem cell-derived neuronal culture [18], CM from primary skeletal muscle cells increased spike and burst rates of primary hippocampal neurons across days (Fig 1A and 1B). The general pattern of development of spike trains over time in RM was consistent with other studies using primary hippocampal cells and primary sensory neurons at a similar cell seeding density [28,29]. Significant differences in spike rates were observed between days ($F_{7, 80}$ = 19.4, $p < 0.001$) and between RM versus CM treatments ($F_{1, 80}$ = 202.2, $p < 0.001$). The interaction between day and treatment was also significant ($F_{7, 80}$ = 23.7, $p < 0.001$). Similar to spike rate, burst rate also showed significant effects of day ($F_{7, 72}$ = 10.5, $p < 0.001$), treatment ($F_{1, 72}$ = 38.3, $p < 0.001$), and interaction between the two ($F_{7, 72}$ = 21.1, $p < 0.001$). The interactions were caused by a different pattern of results for earlier time-points (days 2-7), as compared to later time-points (days 8 and 9). At the early time-points, CM had a higher spike and burst rates, but at later time-points the difference in them between RM and CM was reduced, absent, or reversed.

Fig 1. Functional quantification of neuronal activity measured by an MEA. (A) Normalized spike rate. (B) Normalized burst rate. (C) Synchrony Index. (D) Average muscle contraction amplitudes between control and 10 μM BTS (left). Skeletal muscle contraction patterns in the presence of 0 (top right) and 10 μM BTS (bottom right). Scale bar in x, y: 1 s, 1 μm. (E) Normalized peak fluorescent changes between control and 10 μM BTS. Traces of calcium dynamics in the presence of 0 (top right) and 10 μM BTS (bottom right). Scale bar in x, y: 2 s, 1 $\Delta F/F_0$. Data are represented as mean ± SEM (n = 12 (MEA outcomes of non-BTS group), 6 (BTS group), 3(muscle measurements)). Different lowercase letters indicate significant differences ($p < 0.05$). (F) Raster plots representing spike trains from nine electrodes from RM (top left), RM with BTS (top right), CM (bottom left), and CM with BTS (bottom right) on day 9. Each line and the red box represent a single firing, and synchronous burst, respectively. Scale bar: 2 s.

Similar to spike rate and burst rate, CM also caused neurons to fire more synchronously as compared to RM (Fig 1C). A two-way ANOVA showed a significant effect of day ($F_{7, 75}$ = 175.7, $p < 0.001$), treatment ($F_{1, 75}$ = 4083.4, $p < 0.001$) and the interaction between the two ($F_{7, 75}$ = 231.1, $p < 0.001$). However, unlike spike rate and burst rate which showed greater differences between CM and RM at initial time-points than later time-points, the synchrony index showed the reverse pattern, with greater differences at the later time-points and no difference at the early time-points when little synchronous firing occurred.

Having shown that CM increases spike rate, burst rate and synchronous firing of primary hippocampal neurons in culture, we next wanted to evaluate whether contraction of the muscles was necessary for the MEA effects. The alternative is that muscle cells release neuro-active factors regardless of whether they are contracting. Hence, we repeated the experiment except we treated the muscle cells with a contraction inhibitor before collecting the media. We used a known skeletal muscle myosin II inhibitor, N-benzyl-p-toluene sulphonamide (BTS). BTS weakens myosin's interaction with F-actin and *ex vivo* studies found 10 μM of BTS suppresses force production by 60% [23,24]. Consistent with these results, the amplitudes of muscle contraction were reduced by 69% with BTS *in vitro* (t_4= 20.7, $p < 0.001$; Fig 1D). Moreover, we performed calcium imaging of the skeletal muscles *in vitro* (see details in Materials and methods). Calcium dynamics in muscle cultures show a 73% reduction between control and 10 μM of BTS (t_4= 4.9, p =0.0083; Fig 1E). Widefield (S1 and S2 videos) and calcium imaging (S3 and S4 videos) of skeletal muscles are available as supplementary materials.

BTS prevented CM from increasing spike and burst rate, but had no effect on baseline spike and burst rate in RM. This suggests muscle cell contractions are required for CM to increase spike and burst rate. For spike and burst rate, all factors in the repeated measures ANOVA were significant including day ($F_{7, 212} = 50.2$, $p < 0.001$; $F_{7, 187} = 24.3$, $p < 0.001$), muscle treatment (RM vs. CM) ($F_{1, 31} = 194.0$, $p < 0.001$; $F_{1, 21} = 48.8$, $p < 0.001$), BTS treatment ($F_{1, 31} = 101.2$, $p < 0.001$; $F_{1, 21} = 52.8$, $p < 0.001$) and all interactions (all $p < 0.001$). Post-hoc comparisons showed no difference between RM and RM with BTS ($p = 0.4516$; $p = 0.1607$), whereas CM produced greater spike and burst rates as compared to CM with BTS ($p < 0.001$, $p < 0.001$). Finally, CM with BTS was not different from RM ($p = 0.1272$, $p = 0.9548$) or RM with BTS ($p = 0.4553$; $p = 0.1643$).

While BTS specifically reduced spike and burst rate in CM with no effect on RM, we observed a different result for the synchrony index. BTS completely obliterated the synchrony index when added to either RM or CM treatments. This was supported by a significant effect of day, muscle treatment, BTS treatment and all interactions in the overall repeated measures ANOVA. Post-hoc tests showed that BTS-RM and BTS-CM displayed near zero synchrony across the entire period. The synchrony indices in BTS-RM and BTS-CM groups were significantly lower than RM ($p < 0.001$, $p < 0.001$) and CM without BTS ($p < 0.001$, $p < 0.001$) collapsed across days. Taken together, this suggests BTS has a direct effect on the cell culture preventing synchrony and hence we cannot draw strong conclusions about whether contraction of muscles is required for increasing the synchrony index without further experimentation.

Contracting muscle conditioned media promotes synaptogenesis

Primary hippocampal cells plated in culture form synapses over a period of days. Increased number or strength of synapses could explain the increased synchrony index in CM compared to RM. To quantify synaptic development in response to CM versus RM, we performed immunocytochemistry to count the number of synapses using co-localization of pre- and post-synaptic markers (see details in Materials and methods) on days 2 and 9 for CM and RM [26].

The results showed that CM expedites synaptic development compared to RM. This was supported by a significant effect of day ($F_{1, 20} = 19.6$, $p < 0.001$), no main effect of treatment (RM vs. CM) ($F_{1, 20} = 0.77$, $p = 0.3896$), but a significant interaction between day and treatment ($F_{1, 20} = 8.5$, $p = 0.0087$; Fig. 2A). Post-hoc tests indicated a significant increase in the synapse number from day 2 to 9 in RM ($p < 0.001$), but not in CM ($p = 0.2953$). On day 2, the synapse number in CM was significantly higher by 44 % compared to RM ($p = 0.0145$), but on day 9, no differences between CM and RM were detected ($p = 0.1669$). The confocal images of post-synapses, synaptic vesicles, and colocalization are shown in supplementary materials (S1 Fig).

Fig 2. Morphological quantification of synaptogenesis, synaptic vesicle accumulation, filamentous actin intensity, and astrogenesis. (A) Temporal change in synapse numbers between RM and CM on day 2 and 9. (B) Normalized vesicle accumulation per synapse between RM and CM on day 2 and 9. (C) Normalized F-actin intensity on day 9. (D) Temporal change in astrocyte numbers between RM and CM on day 2 and 9. (E) Confocal images of astrocytes in the cultures on day 2 in RM (left) and CM (right) (S100β, green; DAPI, blue). Scale bar: 50 μm. Data are represented as mean ± SEM (n = 6). Different lowercase letters indicate significant differences ($p < 0.05$).

Contracting muscle conditioned media accrues filamentous actin at presynaptic terminals but does not significantly affect vesicle clustering

Functional synapses display an accumulation of vesicles and filamentous actin at the terminals [30]. F-actin plays a critical role in clustering and transporting vesicles within the synapse [31–34]. Hence, we wanted to determine whether CM affected vesicle accumulation and filamentous actin concentration at the synapse as a potential mechanism for the increased synchrony observed in CM.

Following established methods [26] to quantify neurotransmitter vesicle clustering at the synapse, we measured average intensity of synaptophysin, a transmembrane protein for vesicles, co-localized with Bassoon, presynaptic nerve terminal marker. Results indicated vesicle clustering occurred at a similar rate in CM and RM. The ANOVA indicated a significant effect of day ($F_{1, 20} = 7.6$, $p = 0.0121$), but no main effect of treatment ($F_{1, 20} = 1.1$, $p = 0.2990$) or interaction ($F_{1, 20} = 0.79$, $p = 0.3844$; Fig 2B). On day 2, F-actin was not detected in either CM or RM so results are not shown. However, filamentous actin was detected on day 9 in both groups, and average F-actin intensity in CM was higher by 48% ($t_{10} = 2.9$, $p = 0.0152$; Fig 2C).

Muscle conditioned media from contracting muscles induces astrocyte proliferation

The numbers of astrocytes significantly increased by tenfold from day 2 to day 9 collapsed across RM and CM. CM consistently displayed fourfold greater numbers of astrocytes than RM on both days (Fig. 2D). This was reflected by a significant effect of day ($F_{1, 20} = 145.0$, $p < 0.001$) and treatment ($F_{1, 20} = 49.1$, $p < 0.001$) but no interaction ($F_{1, 20} = 0.93$, $p = 0.3466$). This suggests CM massively increases the proliferation of hippocampal astrocytes similar to the effect observed *in vivo* [16].

Astrocytes regulate neuronal activity *in vitro*

To determine the role of astrocytes in the increased spike rate observed in hippocampal primary cultures exposed to CM versus RM, we repeated the experiment in cultures with reduced astrocyte populations. To remove astrocytes from the primary hippocampal cell culture, we applied a glia inhibitor following established protocols [25] (see details in Materials and methods). Consistent with previous accounts, this resulted in an 81% reduction in the number of astrocytes in the culture (t_{14}= 5.70, $p < 0.001$) (Fig 3A). Confocal images of astrocyte populations in control and astrocyte reduced culture are shown (Fig 3B).

Fig 3. A role of astrocytes as a regulator of neuronal activity. (A) Result of glia anti-mitotic treatment (n = 8). (B) Confocal images of the control and glia reduced culture. Scale bar: 100 μm. (C) Normalized spike rate in the presence and absence of astrocytes. Data are represented as mean ± SEM (n = 18 (unaltered group), 6 (glia reduced group)). Different lowercase letters indicate significant differences ($p < 0.05$). Results for burst rate and synchrony index are shown in supplementary materials (S3 Fig and S1 appendix).

MEA data were collected from normal hippocampal cultures in RM and CM as reference controls, as well as from cultures with reduced astrocytes in RM, CM, Ast-RM, and Ast-CM (see Materials and Methods section on "Collection of muscle and astrocyte media"). In the repeated measures analysis of mean spike rate, all main effects of muscle conditioned media (RM vs CM) ($F_{1, 53} = 254.8$, $p < 0.001$), presence or absence of astrocytes ($F_{2, 53} = 170.6$, $p < 0.001$), and day ($F_{7, 364} = 131.7$, $p < 0.001$) were significant, and all possible interactions between these factors were also significant ($p < 0.001$). The presence or absence of astrocytes factor includes 3 levels, presence, absence, and absence but with the releasate from astrocytes added back in (Ast-RM and Ast-CM groups; see statistical methods). Post-hoc tests indicated that CM increased spike rate relative to RM in normal hippocampal cultures consistent with the previous result ($p < 0.001$), but also in cultures with reduced astrocytes ($p < 0.001$). To our surprise, we found that a reduction of astrocytes increased spike rate in both RM and CM ($p < 0.001$), and the increase in CM with reduced astrocytes was an order of magnitude higher compared to the unaltered culture in CM (Fig 3C). Moreover, the increase in spike rate in CM relative to RM was greater for cultures with reduced astrocytes as compared to unaltered cultures as reflected by the significant interaction between muscle media and presence/absence of astrocytes ($F_{2, 53} = 49.8$, $p < 0.001$). Taken together, these results suggest astrocytes inhibit neuronal activity and CM increases their inhibitory function to counteract the excitatory effect of CM on neuronal activity.

To determine whether astrocytes mediate their inhibitory function through releasing factors into the media or whether they need to be physically present to exert their inhibitory effect, we included the Ast-RM and Ast-CM treatments. In these treatments, astrocytes were removed from the hippocampal culture but media from intact hippocampal cultures with astrocytes was added back in after being exposed to either RM or CM. RM and Ast-CM reduced spike rate relative to RM and CM when the hippocampal cultures were deprived of astrocytes.

Moreover, the spike rate in the Ast- groups was similar to when the astrocytes are physically present in intact primary hippocampal cultures. This is supported by non-significant post-hoc test between groups where astrocytes were physically present versus absent but releasate added back in ($p = 0.0537$). Further, comparisons between normal cultures exposed to CM and astrocyte-deprived cultures exposed to Ast-CM showed no significant difference ($p = 0.9597$). Likewise, normal cultures exposed to RM showed no difference from astrocyte deprived cultures with Ast-RM ($p = 0.68$). These results suggest that astrocytes mediate their inhibitory effect through releasing factors into the media and do not need to be physically present in the culture to exert their influence.

Discussion

Here we establish for the first time an *in vitro* platform to explore interactions between contracting primary muscle cells and primary hippocampal cells. One of the leading hypothesized mechanisms for pro-cognitive effects of exercise is that muscle contractions release factors that cross into the brain where they directly influence hippocampal cells involved in cognition [7,10,14]. This hypothesis is supported by our recent discovery that muscle contractions alone, through electrical stimulation of the sciatic nerve in anesthetized mice, are capable of increasing the generation of new astrocytes in the hippocampus and increasing the volume of the dentate gyrus [16]. The *in vitro* model developed herein adds to this literature by identifying a novel mechanism by which muscle cells may communicate with hippocampal cells. Muscle cells release factors that cause hippocampal neurons to become excited and hippocampal astrocytes to proliferate faster. The expanded astrocytes play a role in regulating neuronal excitability. Together this leads to a network that has overall greater excitability than in absence of the muscle signals, but also greater inhibition from astrocytes. The astrocytes thus tame the increased electrical activation of the circuit from the muscle factors in a way that leads to selective strengthening of coordinated activation patterns between neurons.

A key finding was that muscle contractions are necessary for CM to influence spike rate and burst rate in the hippocampal cultures. When muscles were prevented from contracting by administering BTS, CM no longer produced the increased effects on spike and burst rate (Fig 1A and 1B). This adds important validity to the model since exercise involves mechanical forces and the hypothesis is that muscle contractions release factors that they otherwise would not release to communicate their status of engaging in physical activity to the hippocampus. We were able to make this conclusion because the effect of BTS on spike and burst rate was specific to CM, it had no impact when administered in RM, (i.e., BTS-RM spike and burst rate was similar to RM, but BTS-CM showed reduced spike and burst rate relative to CM). However, this was not true for the synchrony index where BTS appeared to directly eliminate synchronous firing of neurons whether in RM or CM (Fig 1C). Thus, we cannot be certain that the muscle contractions are necessary for the effect of CM on enhancing synchronous firing of action potentials. A method is needed that can prevent the muscle cells from contracting that does not directly interfere with any of the MEA outcomes.

In the context of whole organismal exercise, muscles communicate with hippocampal neurons while hippocampal neurons are involved in the sensorimotor processing in the brain that occurs during physical activity [15,35]. Indeed, acute activation of the hippocampus is strongly correlated with running speed and repeated exercise training increases adult hippocampal neurogenesis and astrogliogenesis [3,5–7]. Together with the *in vitro* data collected herein, the results suggest that muscle contractions contribute to the plasticity in the hippocampus by responding with signals that increase the number of new astrocytes to counterbalance the excitation that is likely intrinsic to the hippocampus involved in the sensorimotor response to physical activity.

Possibly related to the excitation of the hippocampus, whole organismal exercise produces a microenvironment in the hippocampus that is conducive for neurogenesis and synaptogenesis. Consistent with recent reports, results from the present study suggest that signals from muscle contractions likely contribute to the synaptogenic microenvironment. The fact that CM increased maturation of the hippocampal network and increased the formation of mature synapses is consistent with such a role.

It is notable that while CM greatly increased astrogliogenesis, it did not increase neurogenesis in the primary hippocampal cultures. This could be because the stem cell environment was disrupted during the *in vitro* preparation. On the other hand, the lack of an increase in neurogenesis is consistent with the *in vivo* study in which the contribution of muscle contractions was isolated. As mentioned earlier, this study found that repeated electrical contractions of muscles while the animal is anesthetized are capable of increasing astrogliogenesis but not neurogenesis in the hippocampus [16]. Taken together, these results strongly suggest that additional factors besides the muscle releaseate are necessary to increase neurogenesis. This does not rule out the possibility that increased astrocytes and a microenvironment conducive for synaptogenesis may represent support systems signaled by the muscles in anticipation of neurogenesis which usually accompanies whole organismal exercise.

Increased astrocytes could be key to how CM increases synaptogenesis and inhibits neuronal excitability. Astrocytes are well-known homeostatic regulators of neuronal activity. They directly modulate the ratio of excitatory and inhibitory synapses and neurotransmitter concentrations such as GABA and glutamate based on environmental needs. An *in vitro* study found the appearance of GABAergic and glutamatergic synapses by 24 hours when embryonic rat ventral spinal neurons were cultured on astrocytes as compared to 4 and 7 days, respectively in the neuron-only culture [36]. Furthermore, when astrocyte-conditioned media was supplemented in astrocyte-deprived situations, increases in GABAergic synapses, axon length [37], and receptors [38] were detected. Thus, astrocytes appear to release factors that increase GABAergic synapses and do not need to be physically adjacent to neurons to exert their inhibitory influence. This is consistent with their role in our study where media from neuronal cultures with astrocytes was capable of recapitulating the inhibitory effect of astrocytes in a neuronal culture without astrocytes physically present (Fig 3C). It is well established that astrocytes and astrocyte proliferation occur in response to epilepsy, and the evidence suggests astrocytes release factors such as gliotransmitters and tumor necrosis factor-alpha (TNF-α) that inhibit neuronal excitability and are protective against excitotoxicity [39].

In addition to increasing the inhibitory function of astrocytes, CM also increased the maturation of the hippocampal network as reflected in the MEA data and the maturation of synapses. In this study, we used vesicle clustering and F-actin accumulation to quantify mature synapses. The presence of F-actin and vesicles at the terminal of presynaptic neurons is considered an indicator of a mature synapse. Previous *in vitro* studies have used the synaptic vesicle proteins, synapsin I and synaptophysin as markers to track the distribution of

synaptic vesicles during the development of primary hippocampal neuron cultures. The synaptic vesicles change their distribution from being mostly in cell bodies to mostly at synapses as the hippocampal network matures. F-actin is known to be concentrated at presynaptic terminals to support the vesicles [32–34] and to mediate their transportation [31]. Our observation that F-actin is concentrated more at presynaptic terminals in CM than RM implies that CM enhances the maturation of functional synapses with greater capacities to transport vesicles upon action potentials. This could explain why neuronal cultures plated on MEA exposed to CM displayed greater levels of synchronized firings of action potentials than RM because there were more mature synapses.

The increased number of astrocytes in the neuronal cultures exposed to CM may have contributed to the increased maturation of the hippocampal network by strengthening specific synapses and weakening others by pruning and inhibition. Mature synapses appeared earlier and were pruned earlier in cultures with more astrocytes as a consequence of exposure to CM. Whereas synapses continued to increase from day 2 to day 9 in RM, in CM they reached their peak around day 2 and were already in decline by day 9. Astrocyte-secreted proteins such as thrombospondins [40], hevin, and SPARC [41] may have promoted synaptogenesis. Astrocytes can directly eliminate synapses through MEGF10 and MERTK pathways which are two phagocytic receptors detecting signals from silent synapses [42,43].

The *in vitro* model is only useful to the extent that it reflects features of the whole-organismal phenomenon. Whole organismal exercise increases synaptogenesis and astrogliogenesis in the hippocampus and the *in vitro* model displays these features. It is not intended to represent the entirety of exercise's impact on the hippocampus. For example, increased excitability (spike rate, burst rate, synchrony index) of the primary hippocampal network as measured by the MEA has no direct meaning for how neurons behave in the actual hippocampus during exercise. There is no "appropriate" level of excitability, and higher or lower excitability is not any "better" than the other as there is no benchmark for successful performance in a dish. The value of the reduced approach is thus not for recapitulating the patterns of neuronal activity and circuit dynamics, but rather to isolate the effect of muscle factors on basic properties of hippocampal cells.

Before conducting the present studies, we knew astrocytes increased in the hippocampus in response to exercise, and that muscle contraction alone was capable of recapitulating this effect. We observed the same phenomenon of increased astrocytes in the *in vitro* model, which justifies its use for exploring the role of increased astrocytes in the hippocampal response to muscle contractions. Because of the *in vitro* model, we now have a hypothesis for why astrocytes are responsive to muscle factors, they play an inhibitory role in taming the excitability of neurons that occurs in parallel with muscle contractions.

Future studies will build on the *in vitro* platform to explore potential reciprocal communication between muscle cells and hippocampal cells through a co-culture with shared media exchange. We are also interested in using

437 the platform to explore the potential mechanism by which CM causes astrocytes to proliferate and hippocampal
438 networks to mature faster. Finally, we are interested in identifying the bio-active factors released from the
439 contracting muscles that influence the hippocampal cultures. In the future, such information could be used to
440 reverse engineer treatments to recapitulate pro-cognitive effects of exercise in the absence of physical activity.

441

Acknowledgements

We are grateful to Dr. Gelson Pagan-Diaz of the University of Texas for discussions of MEA, Jennie Gardner for general husbandry of animal subjects at the early stage of the study, Md Saddam Hossain Joy for discussions of the double-fluorescent label method, and Carlos Renteria for discussions of calcium imaging and MATLAB code. Lastly, we appreciate Dr. Onur Aydin of the University of Illinois for ideations and insightful discussions of the study.

References

1. Churchill JD, Galvez R, Colcombe S, Swain RA, Kramer AF, Greenough WT. Exercise, experience and the aging brain. Neurobiology of Aging. 2002;23(5).
2. Erickson KI, Kramer AF. Aerobic exercise effects on cognitive and neural plasticity in older adults. Vol. 43, British Journal of Sports Medicine. 2009.
3. Erickson KI, Voss MW, Prakash RS, Basak C, Szabo A, Chaddock L, et al. Exercise training increases size of hippocampus and improves memory. Proceedings of the National Academy of Sciences of the United States of America. 2011;108(7).
4. Clark PJ, Kohman RA, Miller DS, Bhattacharya TK, Brzezinska WJ, Rhodes JS. Genetic influences on exercise-induced adult hippocampal neurogenesis across 12 divergent mouse strains. Genes, Brain and Behavior. 2011;10(3).
5. Clark PJ, Brzezinska WJ, Puchalski EK, Krone DA, Rhodes JS. Functional analysis of neurovascular adaptations to exercise in the dentate gyrus of young adult mice associated with cognitive gain. Hippocampus. 2009;19(10).
6. Redila VA, Christie BR. Exercise-induced changes in dendritic structure and complexity in the adult hippocampal dentate gyrus. Neuroscience. 2006;137(4).
7. van Praag H, Kempermann G, Gage FH. Running increases cell proliferation and neurogenesis in the adult mouse dentate gyrus. Nature Neuroscience. 1999;2(3).
8. Dhikav V, Anand KS. Is hippocampal atrophy a future drug target? Medical Hypotheses. 2007;68(6).
9. el Hayek L, Khalifeh M, Zibara V, Abi Assaad R, Emmanuel N, Karnib N, et al. Lactate mediates the effects of exercise on learning and memory through sirt1-dependent activation of hippocampal brain-derived neurotrophic factor (BDNF). Journal of Neuroscience. 2019;39(13).
10. Trejo JL, Carro E, Torres-Alemán I. Circulating insulin-like growth factor I mediates exercise-induced increases in the number of new neurons in the adult hippocampus. Journal of Neuroscience. 2001;21(5).
11. Fabel K, Fabel K, Tam B, Kaufer D, Baiker A, Simmons N, et al. VEGF is necessary for exercise-induced adult hippocampal neurogenesis. European Journal of Neuroscience. 2003;18(10).
12. Church DD, Hoffman JR, Mangine GT, Jajtner AR, Townsend JR, Beyer KS, et al. Comparison of high-intensity vs. high-volume resistance training on the BDNF response to exercise. Journal of Applied Physiology. 2016;121(1).
13. Moon HY, Becke A, Berron D, Becker B, Sah N, Benoni G, et al. Running-Induced Systemic Cathepsin B Secretion Is Associated with Memory Function. Cell Metabolism. 2016;24(2).
14. Wrann CD, White JP, Salogiannnis J, Laznik-Bogoslavski D, Wu J, Ma D, et al. Exercise induces hippocampal BDNF through a PGC-1α/FNDC5 pathway. Cell Metabolism. 2013;18(5).
15. Delezie J, Handschin C. Endocrine crosstalk between Skeletal muscle and the brain. Vol. 9, Frontiers in Neurology. 2018.
16. Gardner JC, Dvoretskiy S v., Yang Y, Venkataraman S, Lange DA, Li S, et al. Electrically stimulated hind limb muscle contractions increase adult hippocampal astrogliogenesis but not neurogenesis or behavioral performance in male C57BL/6J mice. Scientific Reports. 2020;10(1).
17. McCaig CD. Myoblasts and myoblast-conditioned medium attract the earliest spinal neurites from frog embryos. The Journal of Physiology. 1986;375(1).
18. Aydin O, Passaro AP, Elhebeary M, Pagan-Diaz GJ, Fan A, Nuethong S, et al. Development of 3D neuromuscular bioactuators. APL Bioengineering. 2020 Mar 1;4(1).
19. Wang C, Yue F, Kuang S. Muscle Histology Characterization Using H&E Staining and Muscle Fiber Type Classification Using Immunofluorescence Staining. BIO-PROTOCOL. 2017;7(10).
20. Rando TA, Blau HM. Primary mouse myoblast purification, characterization, and transplantation for cell-mediated gene therapy. Journal of Cell Biology. 1994;125(6).
21. Qu Z, Balkir L, van Deutekom JCT, Robbins PD, Pruchnic R, Huard J. Development of approaches to improve cell survival in myoblast transfer therapy. Journal of Cell Biology. 1998;142(5).
22. Seibenhener ML, Wooten MW. Isolation and culture of hippocampal neurons from prenatal mice. Journal of visualized experiments : JoVE. 2012;(65).

23. Pinniger GJ, Bruton JD, Westerblad H, Ranatunga KW. Effects of a myosin-II inhibitor (N-benzyl-p-toluene sulphonamide, BTS) on contractile characteristics of intact fast-twitch mammalian muscle fibres. Journal of Muscle Research and Cell Motility. 2005;26(2).
24. Cheung A, Dantzig JA, Hollingworth S, Baylor SM, Goldman YE, Mitchinson TJ, et al. A small-molecule inhibitor of skeletal muscle myosin II. Nature Cell Biology. 2002;4(1).
25. Liu R, Lin G, Xu H. An Efficient Method for Dorsal Root Ganglia Neurons Purification with a One-Time Anti-Mitotic Reagent Treatment. PLoS ONE. 2013;8(4).
26. Dzyubenko E, Rozenberg A, Hermann DM, Faissner A. Colocalization of synapse marker proteins evaluated by STED-microscopy reveals patterns of neuronal synapse distribution in vitro. Journal of Neuroscience Methods. 2016;273.
27. Pagan-Diaz GJ, Drnevich J, Ramos-Cruz KP, Sam R, Sengupta P, Bashir R. Modulating electrophysiology of motor neural networks via optogenetic stimulation during neurogenesis and synaptogenesis. Scientific Reports. 2020;10(1).
28. Biffi E, Regalia G, Menegon A, Ferrigno G, Pedrocchi A. The influence of neuronal density and maturation on network activity of hippocampal cell cultures: A methodological study. PLoS ONE. 2013;8(12).
29. Black BJ, Atmaramani R, Kumaraju R, Plagens S, Romero-Ortega M, Dussor G, et al. Adult mouse sensory neurons on microelectrode arrays exhibit increased spontaneous and stimulus-evoked activity in the presence of interleukin-6. Journal of Neurophysiology. 2018;120(3).
30. Fletcher TL, Cameron P, de Camilli P, Banker G. The distribution of synapsin I and synaptophysin in hippocampal neurons developing in culture. Journal of Neuroscience. 1991;11(6).
31. Kim CH, Lisman JE. A role of actin filament in synaptic transmission and long-term potentiation. Journal of Neuroscience. 1999;19(11).
32. Pechstein A, Shupliakov O. Taking a back seat: Synaptic vesicle clustering in presynaptic terminals. Frontiers in Synaptic Neuroscience. 2010.
33. Peng A, Rotman Z, Deng PY, Klyachko VA. Differential Motion Dynamics of Synaptic Vesicles Undergoing Spontaneous and Activity-Evoked Endocytosis. Neuron. 2012;73(6).
34. Pieribone VA, Shupliakov O, Brodin L, Hilfiker-Rothenfluh S, Czernik AJ, Greengard P. Distinct pools of synaptic vesicles in neurotransmitter release. Nature. 1995;375(6531).
35. Saraulli D, Costanzi M, Mastrorilli V, Farioli-Vecchioli S. The Long Run: Neuroprotective Effects of Physical Exercise on Adult Neurogenesis from Youth to Old Age. Current Neuropharmacology. 2017;15(4).
36. Li YX, Schaffner AE, Barker JL. Astrocytes regulate the developmental appearance of GABAergic and glutamatergic postsynaptic currents in cultured embryonic rat spinal neurons. European Journal of Neuroscience. 1999;11(7).
37. Hughes EG, Elmariah SB, Balice-Gordon RJ. Astrocyte secreted proteins selectively increase hippocampal GABAergic axon length, branching, and synaptogenesis. Molecular and Cellular Neuroscience. 2010;43(1).
38. Diniz LP, Tortelli V, Garcia MN, Araújo APB, Melo HM, Seixas da Silva GS, et al. Astrocyte transforming growth factor beta 1 promotes inhibitory synapse formation via CaM kinase II signaling. GLIA. 2014;62(12).
39. Verhoog QP, Holtman L, Aronica E, van Vliet EA. Astrocytes as Guardians of Neuronal Excitability: Mechanisms Underlying Epileptogenesis. Vol. 11, Frontiers in Neurology. 2020.
40. Christopherson KS, Ullian EM, Stokes CCA, Mullowney CE, Hell JW, Agah A, et al. Thrombospondins are astrocyte-secreted proteins that promote CNS synaptogenesis. Cell. 2005;120(3).
41. Kucukdereli H, Allen NJ, Lee AT, Feng A, Ozlu MI, Conatser LM, et al. Control of excitatory CNS synaptogenesis by astrocyte-secreted proteins hevin and SPARC. Proceedings of the National Academy of Sciences of the United States of America. 2011;108(32).
42. Chung WS, Allen NJ, Eroglu C. Astrocytes control synapse formation, function, and elimination. Cold Spring Harbor Perspectives in Biology. 2015;7(9).
43. Chung WS, Clarke LE, Wang GX, Stafford BK, Sher A, Chakraborty C, et al. Astrocytes mediate synapse elimination through MEGF10 and MERTK pathways. Nature. 2013;504(7480).

551
552

Supporting information captions

S1 Fig. Confocal images of synapses. Post-synapses (PSD95) (top) and synaptic vesicle protein (synaptophysin) (bottom) in (A) RM and (B) CM. Orthogonal views of the colocalized channels in (C) RM and (D) CM. Synapses are indicated by the arrowhead. DIV 2. Scale bar: 50 μm.

S2 Fig. Primary skeletal muscle contraction *in vitro*. (A) Myotube with cross-striations indicated by the arrowhead (α-actinin, green; DAPI, blue). Scale bar: 10 μm. (B) Contracting myotube indicated by the arrowhead (left). DIV 6. Scale bar: 100 μm. Contraction pattern of the corresponding muscle fiber (right). Scale bar in x, y: 1 s, 1 μm. (C) Lactate level between RM and CM measured by a colorimetric assay. Data are represented as mean ± SEM (n = 3 (RM), 6 (CM)). Different lowercase letters indicate significant differences ($p < 0.05$).

S3 Fig. Regulation of neuronal activity by astrocytes on MEA. (A) Normalized burst rate. (B) Synchrony index in the presence and absence of astrocytes. Data are represented as mean ± SEM (n = 18 (unaltered group), 6 (glia reduced group)). Different lowercase letters indicate significant differences ($p < 0.05$).

S1 Video. Primary skeletal muscle contraction in the absence of BTS. Scale bar: 50 μm

S2 Video. Primary skeletal muscle contraction in the presence of 10 μM BTS. Scale bar: 50 μm

S3 Video. Calcium dynamics of primary skeletal muscles in the absence of BTS. Scale bar: 100 μm

S4 Video. Calcium dynamics of primary skeletal muscles in the presence of 10 μM BTS. Scale bar: 100 μm

S1 Appendix. Supplementary methods and results

S1 Dataset.

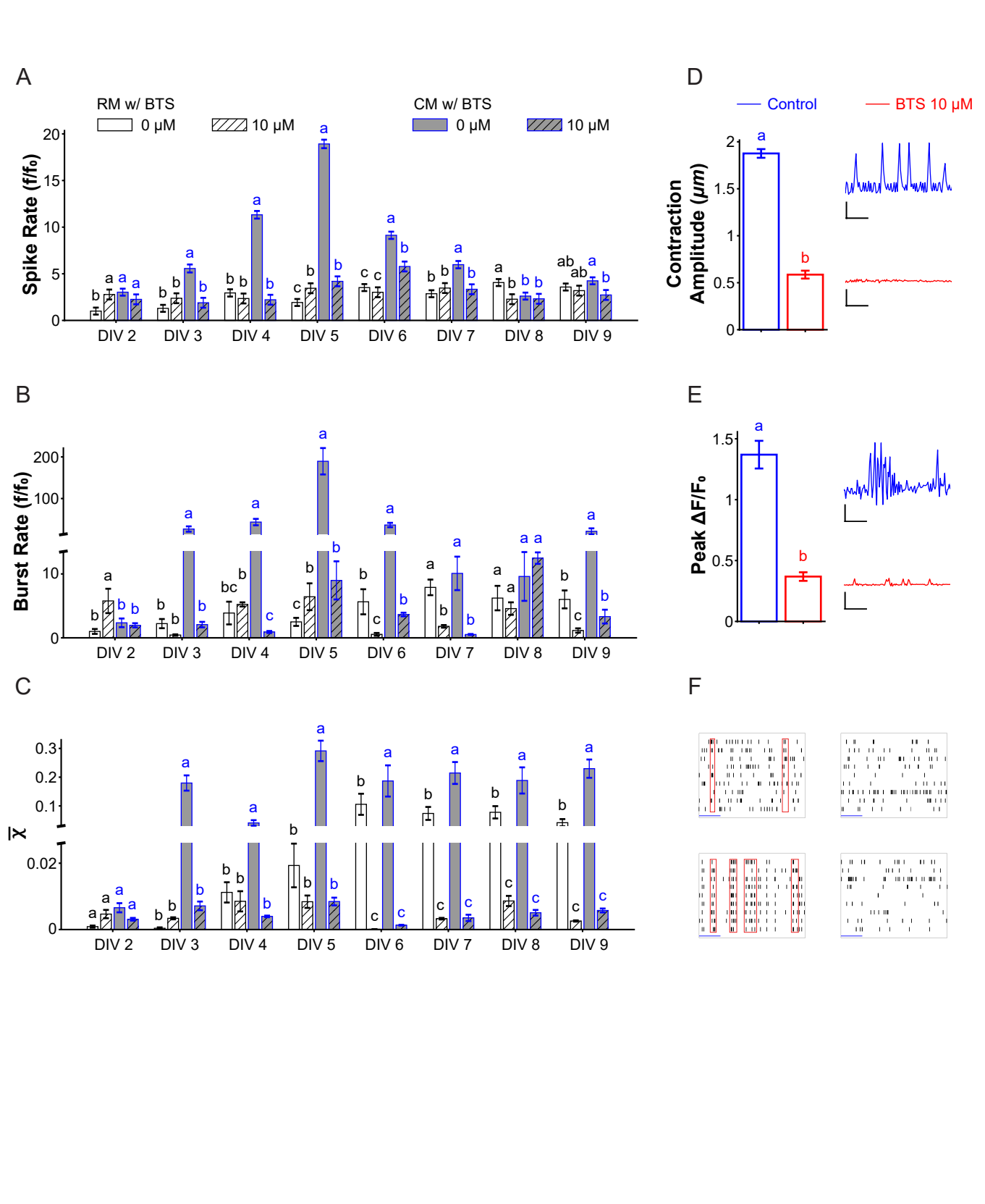
A
RM w/ BTS
0 μM
10 μM
CM w/ BTS
0 μM
10 μM
Spike Rate (f/f₀)
DIV 2
DIV 3
DIV 4
DIV 5
DIV 6
DIV 7
DIV 8
DIV 9
B
Burst Rate (f/f₀)
C
χ̄
D
Control
BTS 10 μM
Contraction Amplitude (μm)
E
Peak ΔF/F₀
F

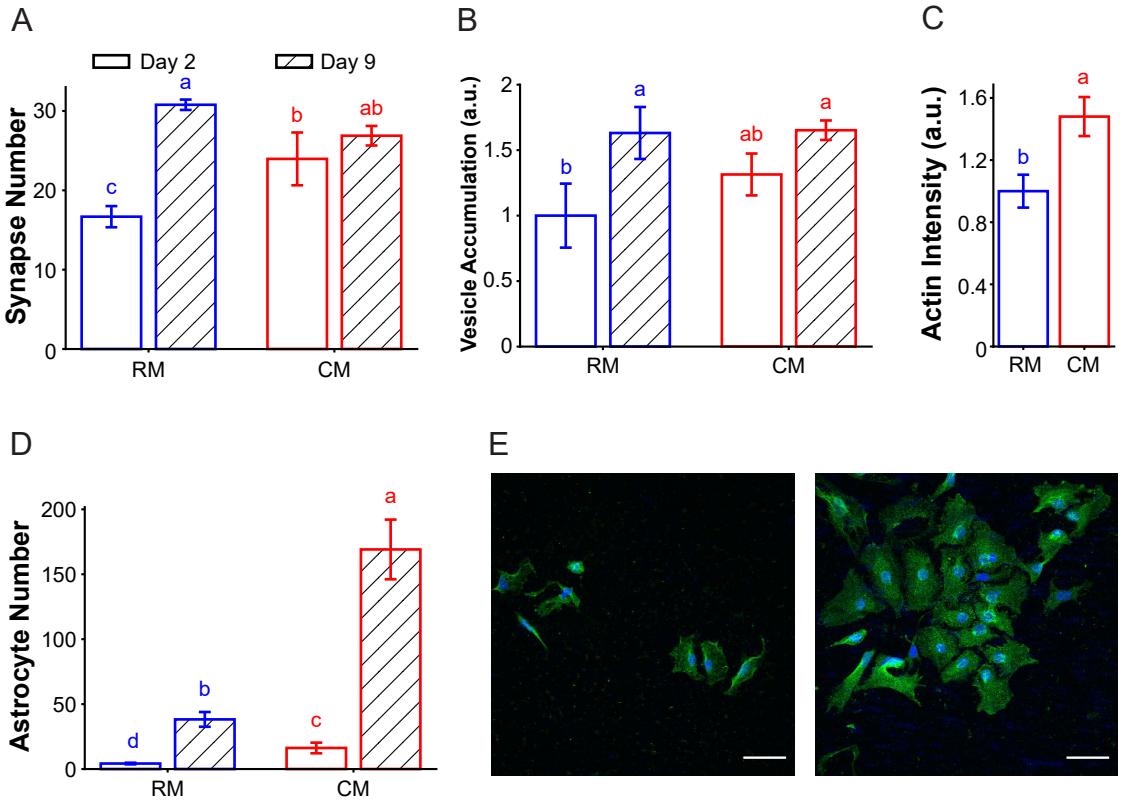
A
Day 2
Day 9
Synapse Number
30
20
10
0
c
a
b
ab
RM
CM
B
Vesicle Accumulation (a.u.)
2
1.5
1
0.5
0
b
a
ab
a
RM
CM
C
Actin Intensity (a.u.)
1.6
1.2
0.8
0.4
0
b
a
RM
CM
D
Astrocyte Number
200
150
100
50
0
d
b
c
a
RM
CM
E

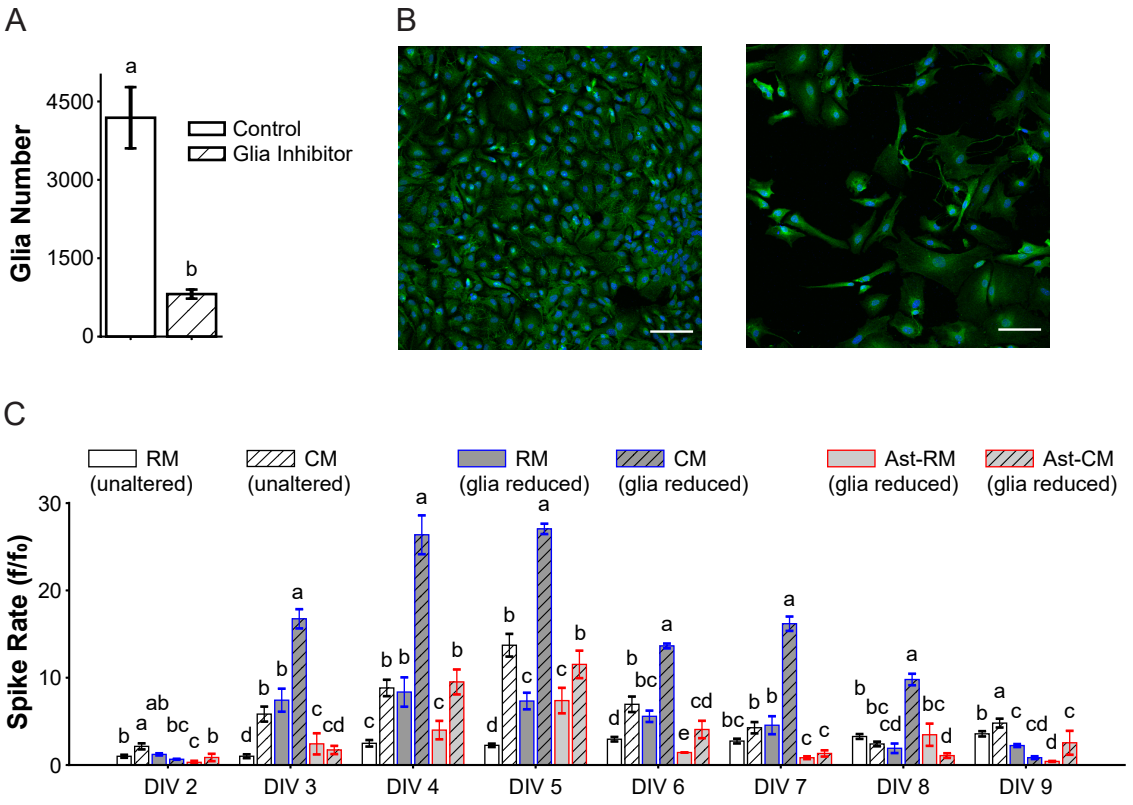
A
B
C
Glia Number
4500
3000
1500
0
Control
Glia Inhibitor
RM (unaltered)
CM (unaltered)
RM (glia reduced)
CM (glia reduced)
Ast-RM (glia reduced)
Ast-CM (glia reduced)
Spike Rate (f/f0)
30
20
10
0
DIV 2
DIV 3
DIV 4
DIV 5
DIV 6
DIV 7
DIV 8
DIV 9